Pergamon

Int. J. Heat Mass Transfer. Vol. 38, No. 8, pp. 1387–1395, 1995

0017-9310/95 $9.50 + 0.00

0017-9310(94)00262-2

Thermal analysis and measurements for a molten metal drop impacting on a substrate: cooling, solidification and heat transfer coefficient

W. LIU, G. X. WANG and E. F. MATTHYS†

Department of Mechanical Engineering, University of California, Santa Barbara, CA 93106, U.S.A.

(*Received* 3 *February* 1992 *and in final form* 2 *August* 1994)

Abstract—The behavior of a molten metal droplet impinging, spreading and solidifying on a solid substrate is relevant to manufacturing processes such as splat cooling and spray deposition. In this study, we have conducted experiments aimed at the investigation of the solidification and cooling of a metal droplet after impact. Temperature measurements were conducted during and after solidification. Some results are presented to illustrate the effect of superheat and substrate material on the cooling rate. We have also estimated the thermal contact coefficient between splat and substrate by matching for a number of conditions the experimental data to predictions of a heat transfer and phase change model. The results suggest that this coefficient can decrease by an order of magnitude during solidification for the case of a splat on metal substrates. For splats on quartz, where there is good bonding, the thermal contact coefficient appears to stay the same before and after solidification.

INTRODUCTION

A common feature of many solidification processes, such as splat cooling, melt-spinning, spray deposition and strip casting, is the removal of thermal energy by contact between the melt and a substrate. Previous analyses [1, 2] confirmed that both the melt thickness and the interfacial heat transfer coefficient between the casting and the substrate are among the most important variables that control the melt cooling and solidification processes. It is therefore essential, if we want to achieve high cooling and solidification rates, to understand and quantify the thermal contact between the melt or solidified metal and the substrate during melt spreading and cooling, melt solidification and solid cooling. In addition, adequate understanding of the thermal contact is important to analyze and predict the possible spallation of the substrate.

When the melt spreads over a solid surface, a perfect thermal contact can not be achieved between the liquid and the solid surfaces because of the roughness of the solid surface, the surface tension of the melt, the impurities on the surfaces, and gas entrapment. As a result, when the melt cools down, crystal nucleation occurs at some discrete locations where the melt is in good contact with the chill substrate and where it has the largest undercooling [3]. In other words, only parts of the surfaces are in true contact when a solid layer forms on the bottom surface of the splat, whereas in other areas the two surfaces are separated by a small gap which may be filled by gas or vapor. Where the solidified metal is in good contact with the substrate, a bond may form between the two, with the strength of the bond depending on the process conditions. If a large number of small gaps exist between the splat and the substrate, a significant thermal resistance may be felt at this interface. In general, a heat transfer coefficient, 'h', is used to quantify the contact between the melt or solidified metal and the substrate. It is therefore expected that the value of h will depend both on the fraction of surface area in good contact and on the reduced heat transfer over the non-contact areas.

Splat cooling, either from a gun or by free fall, has long been used as an effective rapid solidification process to produce new materials with fine microstructures and to study undercooling and solidification kinetics of liquid metals [4, 5]. Many studies have been conducted for splat cooling aiming at the understanding of the final material phases and microstructures produced [4]. Several investigations of the melt spreading and formation of the splat have also been performed [6]. On the other hand, much less attention has been paid to the quantitative analysis of the heat transfer between the splat and the substrate during splat cooling and only limited data are available in the literature on this problem [4].

Two approaches have been used in the past to evaluate h for splat cooling. One approach is to measure experimentally the cooling rate of the splat and then to calculate h by assuming a 'Newtonian' (i.e. no temperature gradient in the splat) cooling condition and

† Author to whom correspondence should be addressed.

NOMENCLATURE

b	splat thickness [μm]
C_P	heat capacity [J kg^{-1} K^{-1}]
H	release height [mm]
h	thermal contact coefficient between splat and substrate [W m^{-2} K^{-1}]
h_1	thermal contact coefficient before and during solidification [W m^{-2} K^{-1}]
h_2	thermal contact coefficient after solidification [W m^{-2} K^{-1}]
k	thermal conductivity [W m^{-1} K^{-1}]
L	latent heat of solidification [J kg^{-1}]
M	drop mass [g]
t	time [s]
t_2	transition time from h_1 to h_2 [s]
T_D	drop temperature upon release [K]
T_M	melting temperature [K].

Greek symbols

α	thermal diffusivity [m^2 s^{-1}]
ε	emissivity of surface of nickel splat
θ	substrate inclination [°]
ρ	density [kg m^{-3}].

Subscripts

L	liquid
S	solid.

a constant temperature substrate [7, 8]. The other technique is based on an indirect approach. First, one measures microstructural parameters such as dendrite arm spacing or eutectic interlamellar spacing, and then one evaluates the melt cooling rate from known or extrapolated relationships between the cooling rate and the relevant microstructure parameter. From this cooling rate one can then estimate the heat transfer coefficient, again assuming a Newtonian cooling condition [4, 9].

In reality, however, after the molten metal contacts the substrate, the substrate surface temperature increases very fast because of the finite thermal diffusion in the substrate and also because of the good thermal contact between the melt and the substrate, and therefore high heat flux [10]. The splat itself may also show significant temperature gradients in some cases, and especially so if a large melt undercooling occurs in the splat, which is possible in particular in the case of gun and drop-squeezing experiments. Indeed, a negative melt cooling rate—i.e. a heating of the melt—may take place during recalescence if a large undercooling exists upon nucleation [2]. The common assumption of isothermal cooling of the splat and constant temperature substrate may therefore result in large errors in the estimated value of h.

It should also be noted that the heat transfer coefficient is not necessarily constant during the entire splat cooling and solidification process. In some cases, for example, the splat may become completely or partially separated from the substrate because of shrinkage during solidification and cooling. The heat transfer coefficient between the splat and substrate may then in principle change significantly after solidification.

More recently, improved techniques have been used to evaluate 'h' between the cast metal and the substrate for planar flow casting [11], strip casting [12], and splat cooling [13]. In these cases, rather than assuming Newtonian cooling, a more realistic heat transfer model is used to derive the interface heat transfer coefficient from the measured temperature data by matching the measured temperature with the model predictions. For example, Ludwig and Frommeyer [11] measured the top surface temperature of an Fe–5wt%Si melt-spun ribbon and then estimated the value of h from the temperature data. Mizukami *et al.* [12] measured the bottom surface temperature of a stainless steel melt ejected from a crucible on a substrate to evaluate the melt undercooling, and also estimated h. Bennett and Poulikakos [13] developed a model for heat transfer during splat cooling of lead droplets and measured the temperature at the interface between melt and substrate with a thermocouple, from which an estimate of the heat transfer coefficient can be calculated as well.

In summary, only limited data can be found in the literature on the interfacial thermal contact coefficient for substrate quenching, and much less so on this coefficient for splat cooling with high-temperature metals. Accordingly, we report in this paper on our investigations of this thermal contact problem for splat cooling of a high melting point metal (nickel) on both metallic and quartz substrates. We have achieved this through the temperature measurement of the splat top surface, which gives us the heat transfer coefficient h by matching with modeling predictions. We also investigated the time-dependent character of interface heat transfer when a nickel droplet impacts on a metallic substrate. The effect of substrate materials as well as other processing parameters was also studied. Given the importance of the interfacial heat transfer on the solidification and cooling rates of a splat, we believe that these results may contribute to the understanding and modelling of the splat cooling and thermal spray deposition processes, as well as provide additional quantitative information on the interfacial heat transfer phenomenon in general.

EXPERIMENTAL SETUP

An electromagnetic induction levitator was used in these experiments in a closed chamber filled with purified argon. The levitator is driven by a 20 kW

Table 1. Material properties used in the calculations

	Unit	Nickel†	Copper‡ (at 400 K)	Aluminum‡ (at 400 K)	St. steel§ (at 473 K)	Quartz‖ (at 973 K)
T_M	K	1726				
L	$J\,kg^{-1}$	2.92×10^5				
C_{PL}	$J\,kg^{-1}\,K^{-1}$	556				
ρ_L	$kg\,m^{-3}$	7900				
k_L	$W\,m^{-1}\,K^{-1}$	50				
α_L	$m^2\,s^{-1}$	1.14×10^{-5}				
ε		0.2				
C_{PS}	$J\,kg^{-1}\,K^{-1}$	616	397	949	530	1205.5
ρ_S	$kg\,m^{-3}$	8900	8933	2702	7900	2200
k_S	$W\,m^{-1}\,K^{-1}$	83	393	240	18	1.94
α_S	$m^{-2}\,s^{-1}$	1.51×10^{-5}	1.11×10^{-4}	9.36×10^{-5}	4.30×10^{-6}	7.31×10^{-7}

† Liquid properties from ref. [20] data at melting temperature; solid properties from ref. [21] at $T = 1500$ K; ε evaluated from ref. [21].
‡ Reference [21].
§ AISI 304 stainless steel [21].
‖ General Electric Catalogue 7700 (April 1986).

power supply. Pure nickel shots were levitated and melted up to a preset temperature and then dropped onto a solid substrate. (We have restricted ourselves to nickel splats in these experiments because of limitation in the pyrometer range.) Two kinds of substrate were used in the experiments: metal (copper, aluminum and stainless steel) and brittle substrates such as fused quartz. The material properties used in the calculations are shown in Table 1. The Ni samples were prepared from 99.9% nickel pellets and arc-melted into small spheres of a size (0.4–1.0 g) suitable for our investigations and for good levitation. The droplet is levitated in an open-bottom quartz tube in which purified argon and helium flow downward. Argon is used to keep the sample free from oxidation, and helium to control and adjust the sample temperature as needed. Two high-temperature IR two-color pyrometers working in the near infrared range (0.7 and 1.07 μm) were used in the experiments, one for the top surface temperature of the splat, and the other one for the initial droplet temperature. Their response time is about 25 ms. The size of the splat area viewed by the pyrometer is about 4–5 mm in diameter for the configuration used, compared to about 15 mm for the entire splat diameter. Figure 1 shows a schematic of the equipment setup. The temperature data for the splat were processed by the pyrometer and recorded on a computer. Some experiments were also run with the substrate placed at an inclined angle in order to achieve more uniform splats. The initial droplet temperatures ranged from 1763 to 2273 K for the metal substrates, and from 1763 to 2073 K for the brittle substrates. The drop height was 265 mm in the vacuum chamber. The metal substrates are all $\frac{1}{2}$ in. in thickness. The surfaces of all metallic substrates were polished with 600 grit abrasive paper before each run. The quartz plates are $2\times2\times\frac{3}{16}$ in. ground and polished.

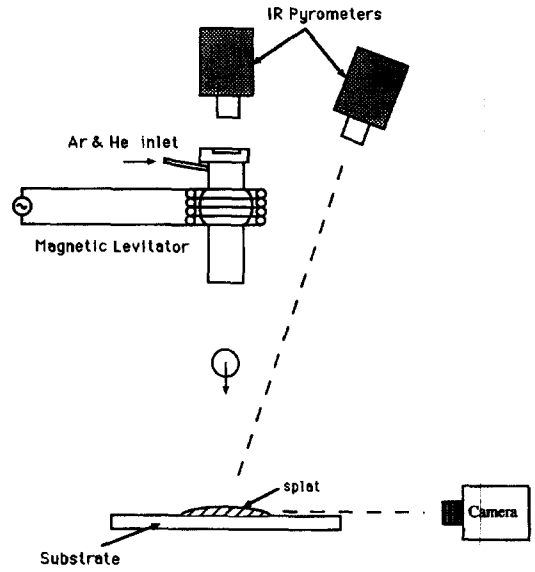

Fig. 1. Schematic of the experimental setup.

NUMERICAL MODEL OF SPLAT COOLING

The heat transfer coefficient between the splat and the substrate has been estimated by matching the measured temperature of the top surface of the splat with results from a one-dimensional heat conduction and phase change numerical model. The formulation and numerical solution procedure used in this model is described elsewhere in detail [14], and only a brief description is given here. The model assumes that, at time $t = 0$, a thin layer of melt at high temperature is suddenly placed in contact with a solid substrate at room temperature. One-dimensional heat transfer is then assumed between the splat and the substrate, with heat transferred from the melt to the substrate by conduction. The convective heat transfer from the

top and side surfaces are negligible compared to conduction to the substrate, but radiation losses from the top surface of splat are included for completeness (they are about 5–10% of the heat transfer to the substrate). We also assume nucleation on the substrate and unidirectional solidification subsequently. Melt undercooling (i.e. a melt temperature lower than the equilibrium melting temperature) prior to solidification is also neglected in these calculations, and the solid–liquid interface within the splat is assumed to remain at the metal equilibrium melting temperature. The thermal conductance between the melt and the substrate due to a non-perfect contact is quantified by a heat transfer coefficient, h. This coefficient, which may be a function of time, is defined as the heat flux between the splat and the substrate divided by the temperature difference between the splat bottom surface and the substrate surface. The heat conduction equations in both the splat and substrate are used together with the solid–liquid interface energy balance condition. By using the boundary conditions and a control volume integral method with an interface-tracking algorithm, one can model numerically the splat cooling problem, including phase change and substrate heating. Given the splat thickness and the initial melt temperature as well as the corresponding material properties, the model can calculate the temperature of the splat top surface as a function of time for any assumed value of h. The splat top surface temperature is then calculated for various values of h, and by comparing these temperatures with those measured experimentally, one can determine the best match, which will give an estimate of the value of h for the experimental conditions of interest.

EXPERIMENTAL RESULTS AND HEAT TRANSFER COEFFICIENT ESTIMATES

In our experiments, the nickel droplet is heated by levitation melting to a preset temperature and is then allowed to fall freely on the substrate at room temperature, where the melt spreads and forms a liquid splat. The superheat of the liquid melt is then transferred to the substrate across the interface between the splat and substrate. The bottom layer of the melt cools down to nucleation temperature at or lower than melting temperature and solidifies. This solidified layer thickens until the whole splat is solidified, and is finally cooled down to close to room temperature. During this process, the pyrometer is aimed at the center of the top surface of the splat and monitors its temperature.

In these experiments, besides the metal substrates mentioned above, we have also investigated the thermal heat transfer behavior of molten nickel droplet impacting on brittle substrates such as quartz. Our interest in these substrates arose from spray deposition processing for metal matrix composites, during which small molten metal particles are sprayed on brittle fibers. It was found that the final composite properties depend strongly on the drop spreading and on the bonding between the metal matrix and the fibers. Among various factors which affect the composite properties, the porosity of the composite, the spallation of the fiber and its coating, and undesirable solidification microstructures are all believed to be related to the melt spreading and subsequent solidification and heat transfer between the melt and the fiber [15]. In our experiments involving molten nickel droplets on quartz, several interesting phenomena were observed, some rather different from what we saw for metal substrates.

For example, it was observed that, when the molten nickel impacts on a metal substrate in this range of conditions, the splats appear thin at the center with thick edges (especially if the melt superheat and the fall height are large) and that the edges appear to curve up and lift off greatly from the substrate. In contrast, the splats on glass or quartz substrates exhibit a central area thicker than the edges. Another difference is the spallation of the brittle substrate resulting from thermal shock and thermal contraction differentials. When a molten nickel droplet impinges on a quartz or glass substrate, the splat will not separate from the substrate at the interface between the splat and the substrate as in the case of the metal substrates. Instead, a fracture will form in the substrate and finally the splat with a spall still attached to it will separate from the substrate. Naturally, this does not happen with the metal substrate. Clearly, both the spreading and the spalling processes are strongly dependent on the heat transfer at the splat–substrate interface which will affect the temperature fields in both the splat and substrate. (Details about our experimental results on spallation of a quartz substrate after impact by a molten nickel droplet will be presented elsewhere.)

In the following sections, we first discuss some typical thermal histories for several melt superheat levels and substrate materials by examining the temperature changes in the top surface of the splat. Then we present our calculated values of the interface heat transfer coefficient, h, for a molten nickel droplet impacting on horizontal and inclined substrates. Finally, the generality and limitations of the measurements and numerical predictions are discussed.

Effects of superheat level and substrate material

Typical measurement data for the splat top surface temperature are shown in Fig. 2 for a molten nickel droplet impacting on a horizontal flat copper substrate. (For better comparison, the thicknesses listed in Figs. 2 and 3 are the thicknesses of the center part of the splat only, because the splats may show a significantly thicker edge at high superheat.) Results for several initial melt temperatures are shown. It is seen that all the splats are cooled down to near melting temperature in less than 0.1 s. For reference, the spreading process was analyzed with high-speed cameras and found to last only a few milliseconds. Except

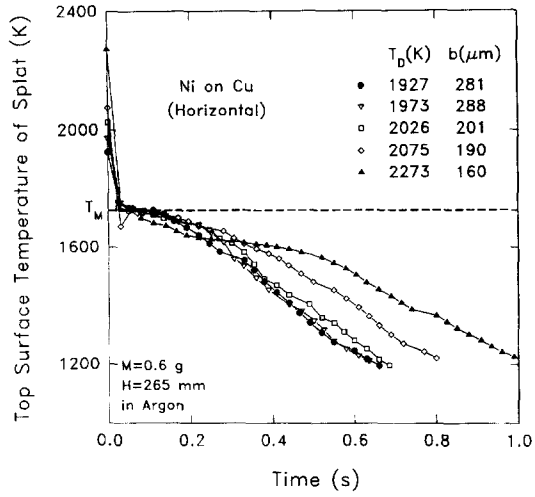

Fig. 2. Top surface temperature of the splat as a function of time. Nickel splat on a horizontal flat copper substrate for several initial melt temperatures (T_D).

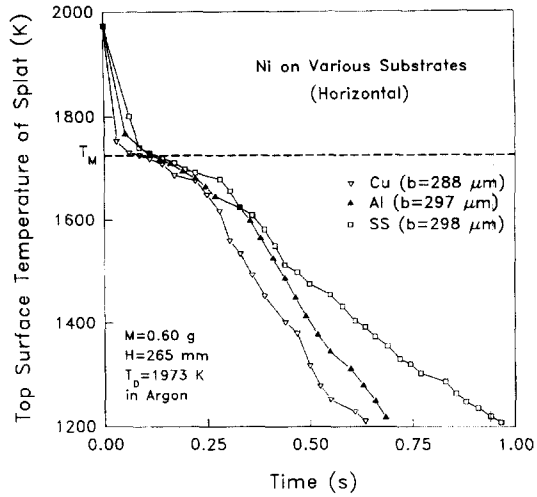

Fig. 3. Top surface temperature of the splat as a function of time. Nickel on three different substrates: copper, aluminum and stainless steel.

for very high initial temperatures, the superheat has only a relatively small effect on the top surface cooling. The pyrometer used in these experiments was too slow to give us many data for the liquid splat, and accordingly we will concentrate hereafter on cooling after solidification. In the experiments shown in Fig. 2, the average cooling rate at the top surface before solidification ranged from about 2500 to 7500 K s^{-1}, and after solidification from 1000 to 500 K s^{-1} for the low and high superheats, respectively. Interestingly, the high superheat splat cooled down slower than the low superheat ones after solidification, even though the thickness of the splats decreases with increasing levels of superheat. This is likely due in part to the fact that the higher the superheat, the higher the temperature of the substrate surface becomes before and during solidification. (See Figure 5 for an illustration of substrate surface heating.) A hotter substrate will then result in slower cooling of the solidified splat.

The influence of the substrate material on splat cooling rate is shown in Fig. 3, which gives the measured temperature of the top surface of nickel splats formed on different substrates: copper, aluminum and stainless steel. The three splats have similar thicknesses for better comparison. It is seen in Fig. 3 that the substrate material has some effect on the splat cooling rate for these conditions of moderate superheat. The splat cools down faster as the thermal diffusivity of the substrate increases (from steel to copper), as expected, but the overall effect of the substrate thermal diffusivity on the cooling rate is not as significant as one might have anticipated based on a ratio of 26 between the thermal diffusivities of copper and steel. In fact, other experiments conducted at lower superheats show very similar cooling rates for all substrates. Likely, this is because the heat transfer resistance across the interface between the splat and the substrate is more of a limiting factor in the overall heat transfer than the conduction in the substrate, therefore masking somewhat the effect of different diffusivities on the latter.

Estimates of the heat transfer coefficient between splat and substrate

As suggested by our examinations of the underside of the splats, the heat transfer coefficient is expected to vary between the center and the edge of the splat, but in this preliminary study we focus only on the center part, with the pyrometer focused on that region. In the following figures and calculations, we are using the average thickness over the entire splat because the splats are fairly uniform in thickness at these low superheat levels, and especially so with inclined substrates. Given the high aspect ratio of these splats, a one-dimensional heat transfer model is expected to be adequate to describe the heat transfer of the splat and of the substrate underneath. Also, as mentioned above, the thermal contact coefficient is not necessarily a constant value but may instead vary with time. In our matching process, we used different values of h before and after solidification in order to obtain the best fit between the experimental data and the numerical results. It was found, however, that a single constant value of h can be used to obtain a relatively good match between the measurements and the numerical results in the case of nickel on a quartz substrate for temperatures above 1200 K (the lower limit of our pyrometer). For metal substrates, on the other hand, at least two distinct values of h have to be used in the model, one before and one after solidification, in order to obtain a good match between the numerical and the experimental data. This difference in thermal contact histories between the two types of substrates is another suggestion of very different bonding and separation mechanisms.

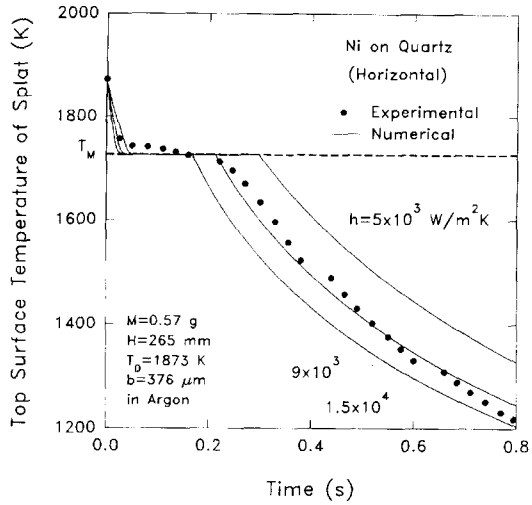

Fig. 4. Matching of numerical model temperature predictions with experimental data for nickel on a horizontal quartz substrate.

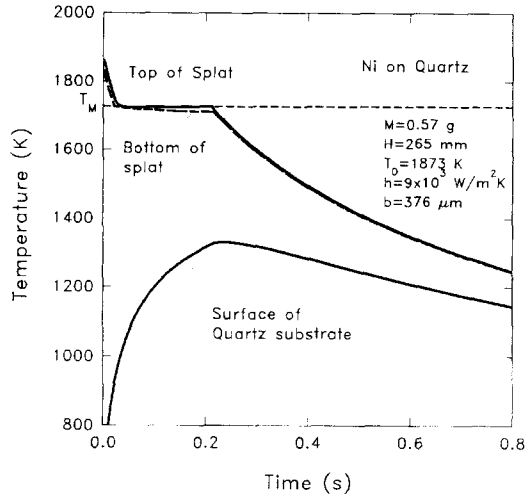

Fig. 5. Calculated temperature histories of the splat top and bottom surfaces and of the quartz substrate surface for the conditions of Fig. 4.

Nickel splat on quartz. Some typical matching results for a molten nickel droplet splatting on a quartz substrate are shown in Fig. 4. In Fig. 4, the dots are experimental temperatures and the solid lines are results of numerical calculation. In this case, the model results match adequately the experimental results before and after solidification with a single value of h, about 9×10^3 W m^{-2} K^{-1}. In Fig. 4, the predicted top surface temperature for two other values of h, 1.5×10^4 and 5×10^3 W m^{-2} K^{-1}, are also given to show the effect of variations in h on the top surface temperature. It was observed that splats formed on quartz substrate resulted in a good bond between the splat and quartz that did not break at large times. Instead, a spall separated from the substrate, still attached to the splat. This spalling separation occurs long after the splat is completely solidified and cooled down to the temperature of 1200 K. In other words, the bond formed between the nickel splat and the quartz substrate is not interrupted above 1200 K, and a constant h can be used to describe the thermal contact condition during this period of time.

Figure 5 shows the calculated temperature histories of both top and bottom surfaces of splat and also of the quartz substrate surface. Given the moderate value obtained for the heat transfer coefficient between splat and substrate (h is about 9×10^3 W m^{-2} K^{-1}), and the relatively high thermal conductivity of the nickel, the temperature gradients in the splat are rather small especially during the solid cooling phase. Interestingly, Fig. 5 also illustrates the high surface temperature of the quartz substrate that are achieved under these conditions. Indeed, the quartz surface temperature would increase to over 850 K in about 17 ms, which is before the melt even starts to solidify. As the melt solidifies, the surface temperature of the quartz surface increases further until it reaches a maximum temperature of about 1340 K, when the solidification is completed. After that, the quartz surface temperature decreases as the solid splat cools down. This rapid increase of the substrate temperature is caused by the fast heat transfer and low thermal diffusivity of the quartz. It is believed that this high surface temperature enhances the bonding between the splat and the quartz.

Nickel splat on horizontal metal substrates. Some typical results for nickel splats formed on horizontal metal substrates are shown in Figs. 6 and 7. Figure 6 shows the results for nickel splatting on an aluminum substrate. In this case, a single value of h is not sufficient to model the experimental results over the whole temperature range. Accordingly, two different values of h, named here h_1 and h_2, are used in the model to obtain a good match between the experimental data

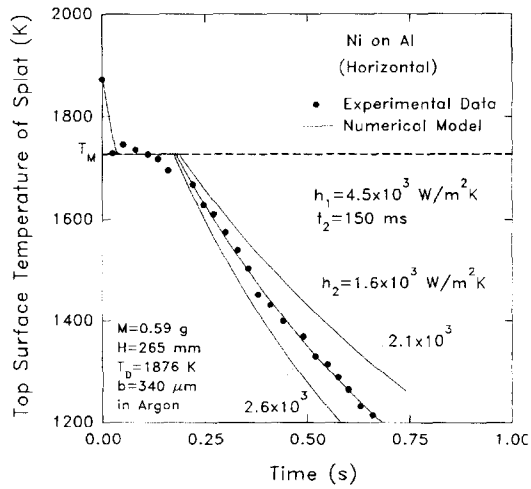

Fig. 6. Matching of numerical model temperature predictions with experimental data for nickel on a horizontal aluminum substrate.

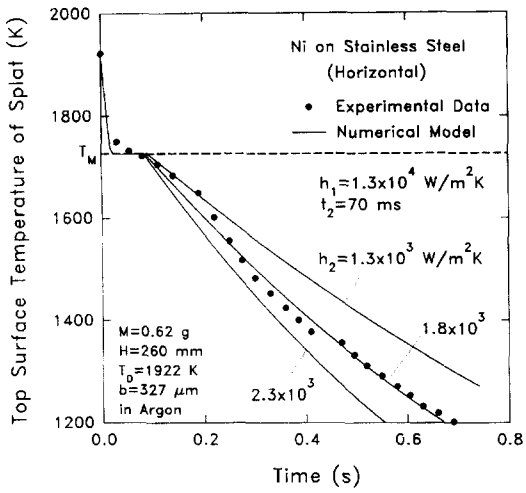

Fig. 7. Matching of numerical model temperature predictions with experimental data for nickel on a horizontal stainless steel substrate.

and the numerical predictions. (The transition time from h_1 to h_2, called here t_2, is determined by best-fit, and is related to the measured solidification time.) The highest value of the heat transfer coefficient, h_1, here about 4.5×10^3 W m^{-2} K^{-1}, is used during the earlier phase when the melt is cooled down and starts to solidify. (Note that we assume in these calculations that the drop impacts the substrate at time $t = 0$ at 10 K less than the release temperature T_D, this calculated temperature drop being due to the convective and radiative heat loss during the free fall of the drop.) After a period of 150 ms chosen for best-fit, a lower value of h_2, 2.1×10^3 W m^{-2} K^{-1}, was used to match the cooling of the solidified splat. In Fig. 6, we show also the numerical predictions for two other values of h_2, in order to illustrate the sensitivity of the matching process on changes in values of h. It is seen that a relatively small change in h_2 (from 1.6×10^3 to 2.6×10^3 W m^{-2} K^{-1}) leads to a large difference in top surface temperature, which indicates that the matching procedure gives good resolution for estimating h. The values of h_1 and t_2 (the transition time) calculated are only rough estimates, however, because of the few data available before and during solidification.

Similar results for nickel on a horizontal stainless steel substrate are shown in Fig. 7. The best-fitting values of heat transfer coefficient in this case are $h_1 = 1.3 \times 10^4$ W m^{-2} K^{-1} and $h_2 = 1.8 \times 10^3$ W m^{-2} K^{-1}. The transition time from h_1 to h_2 used is 70 ms. In Fig. 7 we also show the numerical data for two other values of h_2. It can be seen again that rather large differences in top surface temperature are predicted for a change in h_2 from 1.3 to 2.3×10^3 W m^{-2} K^{-1}. Interestingly, this matching procedure gave us very similar values for the aluminum and stainless steel substrates: 2.1×10^3 and 1.8×10^3 W m^{-2} K^{-1}, respectively, after solidification. The heat transfer coefficient before solidification appears to be significantly higher for stainless steel than for aluminum, however (1.3×10^4 and 4.5×10^3 W m^{-2} K^{-1}, respectively).

For splat cooling on those metal substrates, two values of h have to be used successively in the numerical model in order to get a good match between the numerical predictions and the experimental data. This suggests that the thermal contact condition may change during the cooling process, presumably around solidification time. One would indeed expect that upon solidification and the associated contraction of the bottom surface of the splat, the contact between the splat and substrate will decrease significantly when compared to the liquid–solid contact before solidification. Indeed, in the case of splat on the metal substrates, no significant bonding was observed between the cold splat and the substrate, the splat being unattached after cooling. A macroscopic gap would then lead to a higher thermal resistance at the interface, which is likely seen here as the reduced value of h after solidification.

Nickel on inclined metal substrates. Heat transfer analysis [1, 2] indicates that splat cooling is controlled mainly by two parameters: the thermal contact (i.e. the value of h) and the splat thickness. The accuracy of the estimates for h by the matching procedure based on splat top surface temperature depends therefore on the accuracy of our knowledge of the splat thickness. The thickness of the splat may be fairly irregular in reality, however, especially in the case of metal substrates, but the temperature measured by the pyrometer represents the average value of a relatively small area at the center of the splat top surface.

If it is desired, flatter splats can nevertheless be obtained in order to minimize the uncertainties in h due to thickness measurement errors. This is achieved by inclining the substrate. In this case, the additional melt flow improves the spreading. Our experimental results indeed showed that splats with an irregular thickness and very similar to those obtained on horizontal substrate were formed when the substrate was inclined at a 20° angle from the horizontal. When the substrate is inclined further to an angle of 45°, however, a drop-shaped splat with a very uniform thickness distribution is formed. The resulting splat thickness is also much smaller on this inclined substrate than the average splat thickness on a horizontal substrate (195 microns compared to 271 microns), everything else being the same.

Figure 8 shows the results for a molten nickel droplet released at a temperature $T_D = 1874$ K and impinging on a copper substrate inclined at 45°. The heat transfer coefficients obtained by the matching procedure are 10^4 W m^{-2} K^{-1} for h_1 and 1.9×10^3 W m^{-2} K^{-1} for h_2. It should be noted that the agreement between the experimental data and the predicted values is very good indeed after solidification, which suggests that the thermal contact conditions change little over time at that point. (Note that there is no other adjustable parameter in the model besides h,

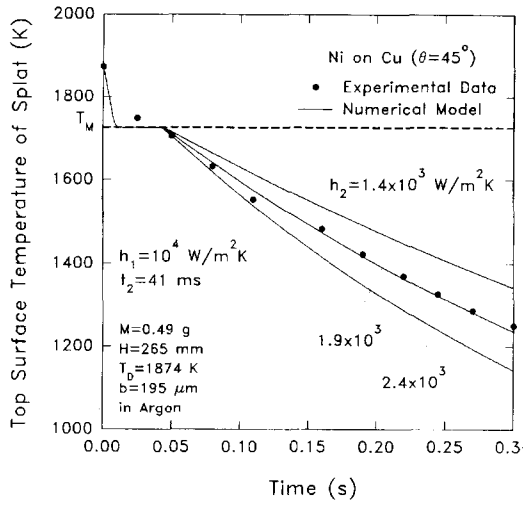

Fig. 8. Matching of numerical model temperature predictions with experimental data for nickel on a copper substrate inclined at 45°.

and that the match between the predictions and measurements was therefore not necessarily guaranteed over such a relatively large range of temperature.) This 'constancy' of h after solidification may lead to some simplifications in the modeling of this process. (Naturally, the heat transfer coefficient may decrease further at very long times after solidification when the splat may undergo macroscopic motion due to large-scale shrinkage.)

Discussion. We should note that, although our estimates of the value of h_2 are probably quite accurate, the values given for h_1 should only be taken as approximate averages. Several reasons lead to the larger uncertainty in h_1. First, only a few temperature data can be acquired during spreading and solidification because of the slow response time of our pyrometer. In addition, the heat transfer process during the spreading process immediately after drop impact is complicated, and can not be well described by a one-dimensional pure conduction model. Even though the matching procedure does not take those issues into account, the values we obtained by this procedure are expected to be in the correct range, as our experience indicates that only a narrow range of value for h_1 can give the correct time at which solidification is completed. For the case of a nickel splat on a copper substrate at 45°, for example (which is believed to give more accurate results because of the flatter splats), we obtained very consistent values for h_1 (1.0×10^4 W m^{-2} K^{-1}) and for the transition times with several different sets of data.

A value of h_1 of about 10^4 W m^{-2} K^{-1} is, in fact, of the same order of magnitude as the initial heat transfer coefficient during melt cooling after ejection of stainless steel on a substrate [12] as well as in free-fall splat cooling of lead [13]. The value we obtained for the cooling of the solid splat—h_2 (about 1.8–3.0×10^3 W m^{-2} K^{-1})—is similar to the h found for larger times during conventional metal mold casting process [16, 17]. The above values of h_2 are also similar to those (1.3–2.6×10^3 W m^{-2} K^{-1}) suggested for twin-belt casters [18]. This is not surprising given the similarity between these processes in terms of thermal contact conditions.

In these calculations, a constant emissivity ($\varepsilon = 0.2$, estimated from measurements with a one-color pyrometer) for the splat top surface was used for the whole cooling process. In reality, of course, the emissivity of the top surface may vary as it changes from a liquid to a solid. The calculations do indicate, however, that during this presolidification period the radiative heat transfer from the top surface to the environment is relatively small compared to the heat flux to the substrate because of the relatively good contact at that time. The uncertainty in emissivity of the top surface will therefore have a small effect on the results. (Results of calculations neglecting this radiative heat loss can also be found in ref. [19], an earlier conference version of this article.) When the nickel droplet is cooling and solidifying on the quartz substrate, a radiative heat loss from the splat bottom surface through the transparent quartz substrate may also exist. Our model does not take into account this heat loss. Examination of the splat bottom surface suggests, however, that this radiation loss is likely small because the splat bottom surface is mirror-like, unlike the top surface, and therefore probably exhibits a smaller emissivity. We believe therefore that the radiation heat transfer at this interface has a negligibly small effect on our calculations.

CONCLUSIONS

A simple experimental setup was used to investigate the solidification, cooling and thermal contact for molten metal droplets impinging on solid substrates. The surface temperature of the splat is monitored by a pyrometer. These measurements allow us to investigate the effect of various processing variables, such as melt superheat, substrate material, splat thickness, etc. on the splat cooling rate. The results indicate that large variations in superheat have only a moderate effect on the splat cooling rate for our range of experimental conditions, with the highest superheat leading to the slowest cooling rate after solidification. Similarly, the effect of substrate material on the splat cooling rate was also found to be small, even for large variations in substrate thermal diffusivity, likely because the thermal contact at the interface between splat and substrate surface becomes the limiting factor in these cases.

The heat transfer coefficient, h, which quantifies the thermal contact at the interface between the splat and the substrate, has been evaluated by matching the experimental measurements of the splat surface temperature with the predictions of a one-dimensional heat conduction model. Some typical matching results suggest the existence of two distinct thermal contact

mechanisms between the splats and the metal substrates. Our calculations show that, for nickel splats on metal substrates, two values of h are needed to model the process: a higher value (about 10^4 W m^{-2} K^{-1} in most cases) before solidification, and a lower value (about 2×10^3 W m^{-2} K^{-1}) after solidification. The numbers reflect the change in thermal contact for liquid–solid to solid–solid as the process takes place. The difference between these two values is rather large in this case: a factor of 5. Interestingly, the use of a time-independent heat transfer coefficient after solidification appears to result in a rather good match between experimental and modelling results, which suggests that the thermal contact does not change much after solidification and until major macroscopic motion of the splat due to thermal contraction takes place. Furthermore, the substrate material was found to have a very small effect on the heat transfer coefficient after solidification: $h = 1.9 \times 10^3$ W m^{-2} K^{-1} for copper; 2.1×10^3 W m^{-2} K^{-1} for aluminum; and 1.8×10^3 W m^{-2} K^{-1} for stainless steel. The calculated coefficients before solidification show a greater span (from 4.5×10^3 to 1.3×10^4 W m^{-2} K^{-1}). These trends are not too surprising, given that the surface tension-controlled contact effects are more likely to be felt when the splat is still liquid, i.e. to be dependent on the substrate material. After solidification, the thermal contact may be controlled much more by the growing small-scale separation between splat and substrate, which is likely to be much more a function of the splat shrinkage than of the substrate, i.e. would be independent of the substrate material, as seen here with a single splat material.

On the other hand, for nickel splat on a quartz substrate, where there is very good bonding between the nickel and quartz, a single value of the heat transfer coefficient—about 10^4 W m^{-2} K^{-1}—is sufficient to model the process before and after solidification. In this case, the bond is strong enough that the splat will not separate from the substrate at the interface, but will rather result in a spall at later times. As the splat stays firmly bonded to the substrate, one would not expect the thermal contact to change appreciably with time, as indeed seen here.

The techniques described here are believed to give us good estimates of the heat transfer coefficient for the splat cooling process. An adequate knowledge of this parameter is indeed essential, not only for analysis of the cooling of the splat itself, but also for the analysis of possible spallation of brittle substrates.

Acknowledgements—We would like to acknowledge gratefully the support of the National Science Foundation (Grant No. DDM-8957733) and of the Defense Advanced Research Projects Agency (Contract No. N00014-86-K-0753); and many valuable discussions with Prof. C. Levi (UCSB).

REFERENCES

1. R. C. Ruhl, Cooling rates in splat cooling, *Mater. Sci. Engng* **1**, 313–320 (1967).
2. G.-X. Wang and E. F. Matthys, Modelling of heat transfer and solidification during splat cooling: effect of splat thickness and splat/substrate thermal contact, *Int. J. Rapid Solidification* **6**, 141–174 (1991).
3. M. Prates and H. Biloni, Variables affecting the nature of the chill zone, *Metall. Trans.* **3**, 1501–1510 (1972).
4. H. Jones, Splat cooling and metastable phases, *Rep. Prog. Phys.* **36**, 1425–1497 (1973).
5. E. W. Collings, A. J. Markworth, J. K. McCoy and J. H. Saunders, Splat-quench solidification of freely falling liquid-metal drops by impact on a planar substrate, *J. Mater. Sci.* **25**, 3677–3682 (1990).
6. G. Trapaga, E. F. Matthys, J. J. Valencia and J. Szekely, Fluid flow, heat transfer, and solidification of molten metal droplets impinging on substrate: comparison of numerical and experimental results, *Metall. Trans. B* **23B**, 701–718 (1992).
7. P. Predecki, A. W. Mullendorf and N. J. Grant, A study of the splat cooling technique, *Trans. AIME* **233**, 1581–1586 (1965).
8. D. R. Harbur, J. W. Anderson and W. J. Maraman, Rapid quenching drop smasher, *Trans. AIME* **245**, 1055–1061 (1969).
9. M. H. Burden and H. Jones, Determination of cooling rate in splat-cooling from scale of microstructure, *J. Inst. Metals* **98**, 249–252 (1970).
10. G.-X. Wang and E. F. Matthys, Modelling of rapid solidification by melt-spinning: effect of heat transfer in the cooling substrate, *Mater. Sci. Engng* **A136**, 85–97 (1991).
11. A. Ludwig and G. Frommeyer, Investigations on the heat transfer during PFC-melt-spinning by on-line high-speed temperature measurements. In *Melt-spinning and Strip Casting* (Edited by E. F. Matthys), pp. 163–171. TMS, Warrendale, PA (1992).
12. H. Mizukami, T. Suzuki, T. Umeda and W. Kurz, Initial stage of rapid solidification of 18-8 stainless steel, *Mater. Sci. Engng* **A173**, 363–366 (1993).
13. T. Bennett and D. Poulikakos, Heat transfer aspects of splat-quench solidification: modelling and experiment, *J. Mater. Sci.* **29**, 2025–2039 (1994).
14. G.-X. Wang and E. F. Matthys, Numerical modelling of phase change and heat transfer during rapid solidification processes: use of control volume integrals with element subdivision, *Int. J. Heat Mass Transfer* **35**, 141–153 (1992).
15. D. G. Backman, E. S. Russell, D. Y. Wei and Y. Pang, Intelligent processing for metal matrix composites. In *Intelligent Processing of Materials* (Edited by H. G. Wadley and W. E. Eckhart, Jr), pp. 17–39. The Minerals, Metals & Materials Society (1990).
16. N. A. El-Mahallawy and A. M. Assar, Effect of melt superheat on heat transfer coefficient for aluminum solidifying against a copper chill, *J. Mater. Sci.* **26**, 1729–1733 (1991).
17. K. Ho and R. D. Pehlke, Metal–mold interfacial heat transfer, *Metall. Trans. B* **16B**, 585–594 (1985).
18. J. K. Brimacombe and I. V. Samarasekera, Fundamental aspects of the continuous casting of near-net-shape steel products. In *Casting of Near Net Shape Products* (Edited by Y. Sahai, J. E. Battles, R. S. Carbonara and C. E. Mobley), pp. 3–24. The Metallurgical Society (1988).
19. W. Liu, G. X. Wang and E. F. Matthys, Determination of the thermal contact coefficient for a molten metal droplet impinging on a substrate. In *Transport Phenomena in Materials Processing and Manufacturing*, Vol. HTD-196, pp. 111–118. ASME (1992).
20. R. I. L. Guthrie, *Engineering in Process Metallurgy*, p. 438. Clarendon Press, Oxford (1989).
21. F. P. Incropera and D. P. DeWitt, *Fundamentals of Heat and Mass Transfer* (2nd Edn), pp. 755–757. John Wiley, New York (1981).